Annals of Science and Technology - A, Vol 11 (1): 41-50, 2026
Copyright: An Official *Journal* of the Nigerian Young Academy
ISSN: 2 544 6320

ARTICLE

Oxybenzone Induced Biochemical Stress and Tissue Alterations in *Clarias gariepinus* and *Oreochromis niloticus*

Germaine A. Ogunwole *, Taiwo A. Ibileye, Efetobor S. Abiya, and Babajide M. Macaulay

Department of Biology, School of Life Sciences, Federal University of Technology, Akure, Nigeria.

Received 28th December, 2025, Accepted 28th May, 2026
DOI: 10.2478/ast-2026-0006

****Corresponding author***

Germaine A. Ogunwole, Department of Biology, School of Life Sciences, Federal University of Technology, Akure, Nigeria.
Telephone: +2347031606728; Email: gaogunwole@futa.edu.ng

Abstract

Oxybenzone (OXB), a common ultraviolet filter in sunscreen products, has raised concerns because of its potential toxicity in aquatic ecosystems. This study evaluated the chronic effects of OXB on oxidative stress, metabolic disruption, and histopathological biomarkers in *Clarias gariepinus* and *Oreochromis niloticus*. Fish were exposed to varying concentrations of OXB spanning 0.1, 0.5 1.0, 1.5, and 2 mg/L for 30 days, after which blood, and liver tissues were retrieved for oxidative stress biomarkers, liver and kidney function indices, glucose levels, and histopathological alterations were evaluated. The result showed that in both fish species, there was significant induction in the activities of superoxide dismutase and glutathione peroxidase than their control counterparts. However, *O. niloticus* exhibited higher baseline antioxidant activity, while *C. gariepinus* experienced greater oxidative damage, as evidenced by its relatively higher lipid peroxidation levels. Liver enzymes such as aspartate aminotransferase, alanine aminotransferase, and alkaline phosphatase were significantly induced in both fishes, although more severe hepatic injury was observed in *O. niloticus*, which was also confirmed histologically. Hyperglycemia was observed in both species, with *C. gariepinus* having the highest relative values with increasing concentration. Urea and creatinine levels was also significantly induced in both species, with *C. gariepinus* also experiencing the most induction. The histopathology analysis in both species revealed liver damage and vascular alterations with varying severity that were specific to both test organisms. This study revealed the potential for OXB to elicit distinct toxicological responses in diverse species, thus, posing ecological risks to freshwater ecosystems.

Keywords: Oxybenzone; Oxidative; Metabolic; Histopathology; *Clarias gariepinus*; *Oreochromis niloticus*.

Introduction

Dating back to the Egyptian civilization in 3000 BC, humans had always desired methods to protect their skin from the tanning effect of the sun (Drissi et al, 2021). The ancient Egyptians utilized rice bran, lupine and jasmine to achieve this desired effect (Drissi et al, 2021). In 1935, the first synthetic Ultraviolet (UV) filters containing benzyl salicylate was released to the public by Eugène Schueller. Subsequently, UV filters became a mainstay in sunscreen products, acting as tiny mirrors, scattering and reflecting UV rays away from the skin. (García-Márquez *et al*., 2024). As a result of the vast usage of UV filters in synthetic sunscreen formulations, its annual global production is estimated to be approximately 10 million tons. Thus, highlighting its significance in the cosmetic industry (Dinardo and Downs, 2021; Marcin and Aleksander, 2023). Furthermore, by 2026, the global sunscreen industry is expected to increase to $13.64 billion (Statista Search Department, 2022; Marcin and Aleksander, 2023). Among these UV filters, oxybenzone (OXB), a derivative of benzophenone, is among the most utilized sunscreen components in cosmetics due to its capacity to absorb UV radiation and provide broad-spectrum photoprotection (Mustieles et al., 2023).

The extensive global use of sunshield agents and its association with fun activities like beach tourism and other swimming events has resulted to its accumulation in marine and freshwater ecosystems, after it must have been rinsed off the skin (Labille *et al*., 2020). Other Indirect sources, include inadequately treated wastewater effluents from treatment plants (WWTPs), which increases their persistence in freshwater and marine environments (Marcin and Aleksander, 2023; Mao *et al*., 2018). The popularity and high demand of OXB have resulted into it been often detected in surface waters and wastewater. It has further been recognized as an emerging contaminant because of its prevalence in aquatic environments (Ortiz-Román *et al*., 2024), with reported concentrations of OXB in waterbodies ranging between 0.7 to 7.8 µg/L. While exceptionally high levels were recorded in the Trunk Bay (1.395 mg/L), Virgin Islands, USA, emphasizing the significant contamination in high tourism coastal regions (Ortiz-Román *et al*., 2024; Downs *et al*., 2016). A study by Bratkovics *et al*. (2015), revealed that OXB concentration varies seasonally, with peak values recorded during the summer months and lesser values recorded during the winter. This is likely due to warmer temperatures and greater outdoor recreational activities in the summer, than what is obtainable during the winter characterized by extreme cold weather, fewer outdoor activities, and lesser sunscreen use.

Ecotoxicological concerns of OXB have led to it ban in regions like Hawaii (Suh *et al*., 2020) and Thailand (Chatzigianni *et al*., 2022). In the marine ecosystem, the active compounds present in sunscreen formulations have been reported to contribute to coral bleaching through multiple pathways. These pathways include the induction of genotoxic effects, endocrine system interference, oxidative stress generation, photosynthetic inhibition, enhanced pathogen vulnerability, and amplification of thermal stress responses (Thomas *et al*., 2024). These physiological challenges often acting synergistically further impair coral homeostasis. Ultimately triggering the expulsion of endosymbiotic zooxanthellae, and subsequently leading to the distinctive whitening appearance associated with coral bleaching (Thomas *et al*., 2024). Sunscreen chemicals such as OXB and Octocrylene (OCT) induce acute and multigenerational toxicities in fish, which results to genotoxicity, developmental defects, and diminished reproductive fitness (Zhou *et al*., 2022; Zhao *et al*., 2023). Their endocrine disrupting effects in fish also lead to skeletal malformations, male feminization, thyroid dysfunction, and behavioral alterations (Tao *et al*., 2023). In aquatic invertebrates, several studies have reported cases of analogous transgenerational impacts alongside disrupted biomineralization, which disrupts shell/exoskeleton formation in corals and bivalves (Santonocito *et al*., 2020; Pham *et al*., 2022).

Diverse research on OXB have predominantly focused on marine environments, leading to its classification as a marine pollutant, perhaps, largely due to its broad use in sunscreens and documented toxicity to corals and marine fauna (Chatzigianni et al., 2022). Research on freshwater ecosystems remains comparatively low, with most studies employing zebrafish (*Danio rerio*) as the primary model organism (Bai et al., 2023; Wang et al., 2023; Ortiz-Román et al., 2024). While zebrafish provide important insights, reliance on a single model may limit understanding of OXB's effects across the diversity of freshwater species. To address this gap, the current study employs the African Sharp-toothed catfish (*Clarias gariepinus*) and the Nile tilapia (*Oreochromis niloticus*). These fishes are ecological and economical significant species with distinct habitat preferences and physiological traits. *C. gariepinus*, is a benthic detritivore, which provides insights into pollutant interactions in sediment laden environments, while *O. niloticus*, which is a pelagic filter feeder, reflects the risks to species critical to global aquaculture. By expanding the taxonomic scope, this research aims to shed more light on interspecies variations in OXB sensitivity, and refine risk assessments for freshwater biodiversity. Therefore, this study aims to evaluate OXB-induced oxidative stress (superoxide dismutase [SOD], glutathione peroxidase [GPx] and lipid peroxidation [LPO]), liver damage (alanine aminotransferase [ALT], aspartate aminotransferase [AST], and alkaline phosphatase [ALP]), and metabolic disruptions (glucose, creatinine, and urea) in *C. gariepinus* and *O. niloticus* at environmentally relevant concentrations.

Methods

Test Chemical and Preparation of Stock Solution

Oxybenzone (OXB), a pale yellowish crystalline solid (melting point, 62-65°C), was obtained from Delson Pascals Ventures Ltd., Akure, Nigeria. A stock solution was prepared by dissolving 1 g of oxybenzone in 1 L of distilled water. Serial dilutions of this stock solution were then made using distilled water to obtain working solutions at concentrations of 0.1, 0.5, 1.0, 1.5, and 2 mg/L.

Experimental Design and Animal Acclimatization

The approval for this study was granted by the Federal University of Technology, Akure, local ethics commission with number (FUTA/ETH/24/190). All procedures involving *C. gariepinus* and *O. niloticus* were conducted in accordance with internationally accepted ethical guidelines for the care and use of laboratory animals. One hundred juvenile *C. gariepinus* ([mean total length = 13.5 ± 0.3 cm; body weight = 42-51 g]) and one hundred juvenile *O. niloticus* ([mean total length = 11.50 ± 0.3 cm; body weight = 33- 40 g]) were obtained from a fish farm in Ibadan, Nigeria, and acclimatized following the protocol described by Ogunwole et al. (2024). Upon arrival, fish were initially housed in aerated glass tanks with water from the collection site for 24 hours for stabilization, followed by a ten days acclimatization period in chlorine free tap water under laboratory conditions (temperature: 30 ± 2°C; pH: 7.0 ± 0.2; DO > 6 mg/L). Active Fish of uniform size and weight within the specified ranges, exhibiting no signs of disease, stress or physical damage, were randomly selected for the experiment. Fish were fed 2 mm Crowns commercial fish feed twice daily at 3% body weight, and about 80% of the tank water was siphoned daily to eliminate feed debris and metabolic waste which may induce stress in the test animals.

For the bioassay, twenty-eight 10 L glass aquaria (32.3 × 21.5 × 14.5 cm) were prepared, each containing 7 L of dechlorinated water. Fish were randomly assigned to five sublethal OXB concentrations (0.1, 0.5, 1.0, 1.5, and 2 mg/L), and a control that had only dechlorinated tap water. T
hese concentrations were selected to mirror environmentally relevant levels and worst-case contamination scenarios. The lowest concentration (0.1 mg/L) exceeds the commonly reported environmental range (0.7-7.8 µg/L: (Balmer et al., 2005; Ortiz-Román et al., 2024) but remains within an order of magnitude of real-world high-exposure cases. The 1 mg/L treatment closely aligns with the extreme contamination recorded in Trunk Bay (1.395 mg/L: Downs et al., 2016; Ortiz-Román et al., 2024), making it a relevant reference point for extreme pollution events. Higher concentrations (1.5 and 2 mg/L) were included to model potential pollution spikes in areas with high sunscreen use, untreated wastewater discharge, or restricted water flow. This range ensures a good assessment of the toxic effects of broad contamination in freshwater species. Each treatment was replicated with five fish per tank, resulting in a stocking density of 30 - 50 g/L, this range is considered acceptable for short-term studies with juvenile fish under controlled conditions. The experiment lasted for 30 days, with the test solutions replaced every 24 h to minimize chemical adsorption and maintain consistent exposure levels. After 30 days, the fish were Immobilized using 150 mg/L tricaine methanesulfonate (MS-222) and sodium bicarbonate buffer, until opercular movement ceased, followed by euthanasia via cervical dislocation. Blood and liver tissue was collected immediately post-euthanasia. With the help of the heparinized 21-gauge syringes, blood was drawn from the inter pelvic region of experimental and control fish and preserved in EDTA anticoagulant tubes. The liver samples were carefully excised, rinsed with phosphate-buffered saline (PBS, pH 7.4), rapidly stored at 4 °C, and then immediately processed for biochemical and histopathological analysis.

Oxidative Stress Assays

Frozen liver tissue was processed under chilled conditions using 0.1 M phosphate buffer (pH 7.4) at a 1:5 tissue-to-buffer ratio using a high-speed rotor-stator homogenizer. Homogenates were centrifuged at 10,000 × g for 15 minutes at 4°C for SOD assays, and at 3,000 × g for 10 minutes at 4°C for GPx and MDA assays. Supernatants were used for biochemical analyses.

Superoxide Dismutase (SOD) activity was determined by its ability to inhibit epinephrine auto-oxidation, measured at 480 nm, as described by Ikumawoyi et al. (2016). The reaction solution (3,000 µL) included 2,950 µL sodium carbonate buffer (pH 10.2), 20 µL liver homogenate, 30 µL epinephrine, and 0.02 mL water. Absorbance changes at 480 nm were monitored over 5 minutes to determine enzyme activity. The activity of Glutathione Peroxidase (GPx) was measured following the procedure described by Adeyemi et al. (2022). A 500 µL aliquot of tissue homogenate containing protein was incubated with 100 µL of reduced glutathione (GSH), 100 µL of hydrogen peroxide (H_2O_2), 100 µL of sodium azide (NaN_3), and 0.1 M phosphate buffer (pH 7.4), bringing the total reaction volume to 2,500 µL. The reaction mixture was maintained at 37°C for 10 minutes. To end the enzymatic activity, 2,000 µL of orthophosphoric acid was added, followed by centrifugation at 3,000 × g for ten minutes at 4°C. The resulting supernatant was combined with sodium hydrogen phosphate (Na_2HPO_4) and DTNB, and the absorbance was recorded at 412 nm after incubation for ten minutes at 37°C. A control without enzyme activity was included to account for non-enzymatic reactions. Malondialdehyde (MDA), a lipid peroxidation marker, was quantified using the method of Nwabueze et al. (2020). TCA-TBA-HCl reagent was added to 1 mL of supernatant, and the mixture was heated at 100°C for 15 minutes. Following cooling at 4°C and centrifugation at 3,000 × g for 10 minutes, the absorbance was measured at 532 nm. Using an extinction coefficient of 1.56×10^5 $M^{-1}cm^{-1}$, the MDA concentration was then estimated.

Liver Function Parameters

Obtained blood plasma was centrifuged at 3,000 × g for 10 minutes. Activities of aspartate aminotransferase (AST) and alanine aminotransferase (ALT) were estimated spectrophotometrically using the methods described by Dorcas and Solomon (2014). This was done by tracking the formation of hydrazone products through reactions with 2,4-dinitrophenylhydrazine. The alkaline phosphatase (ALP) activity in plasma was likewise measured spectrophotometrically following the method of Esenowo et al. (2022). Three cuvettes (Macro, Semi-micro, and Micro) were prepared, with plasma volumes of 50 µL, 20 µL, and 10 µL, respectively. Reagents were then added in volumes of 3,000 µL, 1,000 µL, and 500 µL to the corresponding cuvettes. Thereafter, the solution was thoroughly mixed, and the initial absorbance was determined at 405 nm using a mercury lamp at 37°C. Three measurements were recorded at one-minute intervals. ALP activity was then calculated using the formula: U/L = 2,760 × Absorbance at 405 nm / Minute.

Metabolic Parameters

Glucose level in the plasma were determined using the O-toluidine method, as previously outlined by Clara-Bindu et al. (2021). The supernatant was treated with O-toluidine reagent before undergoing a heating and cooling cycle. The chromogenic reaction product was then quantified spectrophotometrically at 630 nm. Creatinine was quantified in plasma using the Jaffe method, as described by Ziaei-nejad et al. (2021). Working reagent, standard, and sample were prepared, their absorbance was recorded at 500 nm after 30 and 90 s. Plasma creatinine levels were expressed in mg/dL. Urea levels were determined in plasma using the Nesselerization method (Ajeniyi and Solomon, 2014). Test tubes (blank, standard, sample) were prepared with working reagent and distilled water, incubated for 10 minutes, and absorbance measured at 340 nm. Plasma urea levels were expressed in mg/dL.

Histological Preparation, Tissue Processing, and Embedding

Formalin-fixed liver tissues underwent processing in an automated tissue processor (Microm STP 120, Thermo Fisher Scientific, USA) with the following schedule: an initial 1-hour fixation in NBF; dehydration in 70%, 90%, and 95% ethanol, each for 2 hours; two 2-hour changes of 99.8% ethanol; two 2-hour changes of xylene for clearing; and three 2-hour infiltrations with paraffin wax at 60°C. The processed tissues were then embedded in paraffin blocks using an automated embedding center. With a rotary microtome (Microm HM 325, Thermo Fisher Scientific, USA), Tissue sections of 4 µm thickness were prepared from paraffin blocks and stained following the protocol described by Avwioro (2014). Briefly, dewaxed and rehydrated sections (xylene → graded ethanol → water) were stained with hematoxylin (10 min), differentiated (1% acid alcohol), and counterstained with eosin Y (2 min). After dehydration (ethanol series) and clearing (xylene), slides were DPX-mounted. Stained sections were imaged using an Olympus CX41 microscope with E-PM2 camera and analyzed in ImageJ (v1.53t).

Statistical Analysis

Excel 2021 was used to organize the biochemical data, which were then analyzed with SPSS version 23.0. Treatment group means were compared via one-way ANOVA, with Duncan's Multiple Range Test used for post-hoc analysis when significant differences were identified ($p<0.05$).

Results

Hepatic Antioxidant Response and Oxidative Stress Biomarkers

Figure 1 shows hepatic superoxide dismutase (SOD) activity in *Clarias gariepinus* and *Oreochromis niloticus* following exposure to OXB (0.1–2.0 mg/L). SOD activity rose significantly ($p < 0.05$) in both species across all concentrations when compared to the control group. In both species, there was a clear induction of SOD with increasing concentration, with the 2.0 mg/L group recording the highest SOD activity ($p < 0.05$). Overall, *O. niloticus* displayed consistently higher induction of SOD activity than *C. gariepinus*, and its SOD response at 2.0 mg/L was also more pronounced. Figure 2 depicts the hepatic glutathione peroxidase (GPx) activity in *C. gariepinus* and *O. niloticus*. In *C. gariepinus*, fish exposed to all concentrations of OXB displayed significant increases in the levels of GPx activity than their control counterpart, but statistically did not differ among themselves. In contrast, *O. niloticus* exhibited a robust induction of GPx activity with increasing concentration, with each OXB concentrations exceeding that of the control group. The control group remained the lowest, while the 2 mg/L group attained the highest GPx activity.

As shown in Figure 3, lipid peroxidation (LPO), measured as nmol MDA/g, increased significantly ($p < 0.05$) in both species with rising OXB concentrations, relative to the control. In both species, fish subjected to 0.1 mg/L showed the lowest LPO level, whereas the 2 mg/L group showed the greatest elevation. Notably, whereas SOD activity was generally higher in *O. niloticus*, LPO increases were more pronounced in *C. gariepinus*.

Hepatic Enzymatic Activity

Hepatic aspartate aminotransferase (AST) activity (Figure 4) rose significantly in both species with increasing OXB concentration ($p < 0.05$) compared to the control group. In *C. gariepinus*, lower OXB doses (0.1–1 mg/L) did not differ from one another but all exceeded the control ($p < 0.05$). Higher concentrations (1.5–2 mg/L) caused a further significant rise in AST. Similar to *C. gariepinus*, *O. niloticus* also revealed significant increases in ALT level in the exposed fish, with the highest dose (2 mg/L) inducing the greatest elevation ($p < 0.05$). Across comparable treatments, *O. niloticus* generally displayed higher AST values than *C. gariepinus*.

Figure 5 illustrates hepatic alanine aminotransferase (ALT) activity, ALT increased significantly ($p < 0.05$) in both species with rising OXB concentrations. In both species, ALT activity was significantly inhibited in fish exposed to OXB concentrations raging between 0.1–1.5 mg/L. However, there was reverse in fish exposed to the highest concentration (2 mg/L), with ALT activity being significantly higher than in the rest of the groups. Overall, *O. niloticus* showed slightly higher ALT activity than *C. gariepinus* under similar treatments.

Figure 6 shows hepatic alkaline phosphatase (ALP) activity, which rose significantly ($p < 0.05$) in both species in response to higher OXB concentrations of 1.5 – 2 mg/L. In contrast, ALP activity in lower concentrations of 0.1 – 1 mg/L were significantly lower than those observed in the control group. Overall trend showed that *O. niloticus* exhibited slightly higher ALP activity than *C. gariepinus* at the top two concentrations (1.5–2 mg/L).

Metabolic and Renal Biomarkers

Hepatic glucose concentrations in both species (Figure 7) increased significantly ($p < 0.05$) and generally in a concentration-dependent manner under OXB exposure, with the highest peak recorded in the 2 mg/L group. Furthermore, the level of hyperglycemia in *C. gariepinus* was notably higher than *O. niloticus.*

As shown in Figure 8, creatinine levels in both *C. gariepinus* and *O. niloticus* rose significantly ($p < 0.05$) in fish exposed to 1 – 2 mg/L of the test compound. In contrast, lower OXB concentrations of 0.1 mg/L and 0.5 mg/L revealed significant lesser levels of creatinine than those in the control group. In both species, the lowest and highest creatinine level was recorded in fish exposed to 0.1 and 2 mg/L, respectively. Generally, *C. gariepinus* had higher creatinine values than *O. niloticus* under comparable conditions.

There was a progressive increase in urea levels with increasing concentration of OXB in both species. In similar fashion to creatinine, *C. gariepinus* exhibited slightly higher urea levels than *O. niloticus* at comparable exposures (Figure 9).

Liver Histopathology

Histopathology analysis of liver sections from *C. gariepinus* and *Oreochromis niloticus* revealed distinct differences in tissue architecture between the control and experimental groups (Plate 1). In the liver sections of the control group of *C. gariepinus* (Plate 1a), a normal hepatic architecture was observed with the presence of intact and well organized portal veins (PV). However, liver sections from the experimental group exhibited varying degrees of tissue damage, including necrosis (N), melano macrophage center (MMC) formation, periportal edema (PE), blood congestion (BC), and mild steatosis (MS), as well as patch degeneration (PD) (Plates 1b-e).

For *Oreochromis niloticus*, the control liver (Plate 1f) showed a typical central vein (CV) arrangement with no pathological changes. In contrast, liver sections from the experimental group displayed diffuse hepatocyte congestion (DHC), mild steatosis (MS), and extensive fibrosis (EF) (Plate 1g-h). Further tissue damage that was recorded included periportal edema (PE), blood congestion (BC), and coagulative necrosis with hemorrhage (CNH) (Plate 1i). Furthermore, additional signs of periportal edema (PE), mild necrosis (N), and severe necrosis (SN) were recorded (Plate 1j).

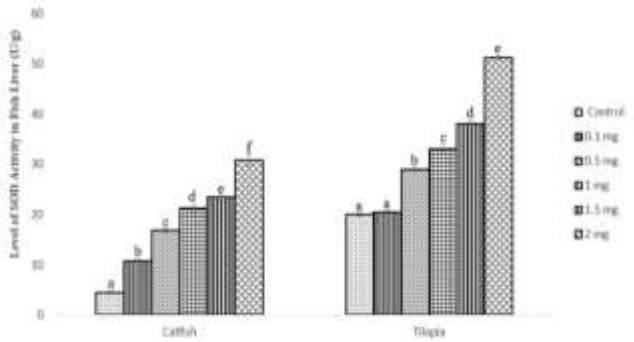

Figure 1: Superoxide Dismutase Activity in the Liver of *Clarias gariepinus* and *Oreochromis niloticus* Following Exposure to Oxybenzone.

Note: Values sharing identical superscript letters are considered statistically similar

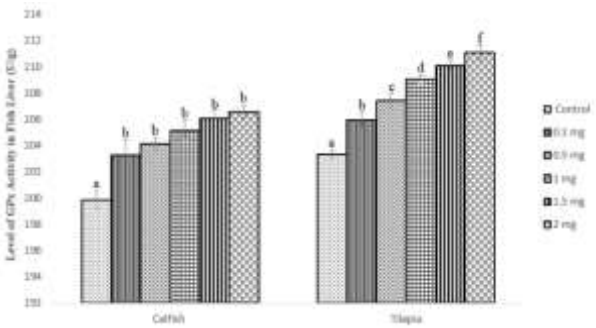

Figure 2: Glutathione peroxidase Activity in the Liver of *Clarias gariepinus* and *Oreochromis niloticus* Following Exposure to Oxybenzone.

Note: Values sharing identical superscript letters are considered statistically similar.

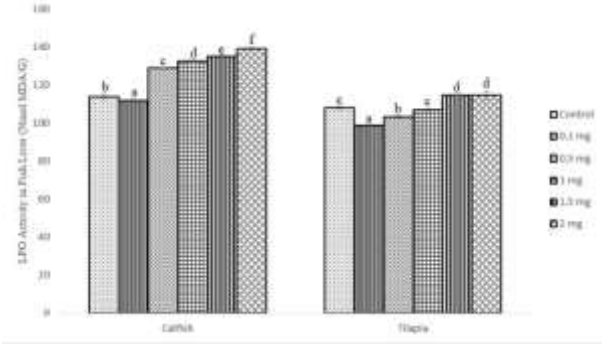

Figure 3: Lipid Peroxidation (LPO) Levels in the Liver of *Clarias gariepinus* and *Oreochromis niloticus* Following Exposure to Oxybenzone.

Note: Values sharing identical superscript letters are considered statistically similar

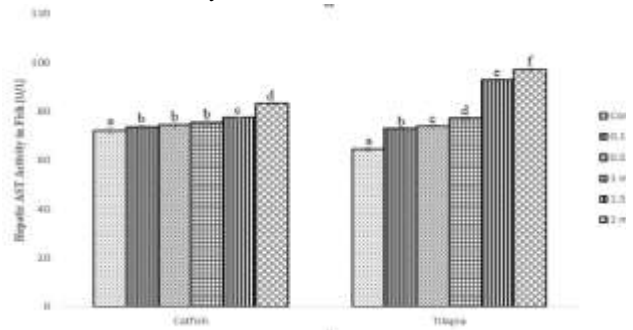

Figure 4: Hepatic Aspartate Aminotransferase Activity in *Clarias gariepinus* and *Oreochromis niloticus* Following Exposure to Oxybenzone.

Note: Values sharing identical superscript letters are considered statistically similar.

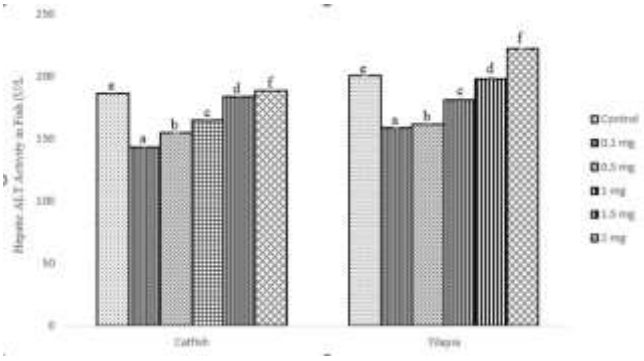

Figure 5: Hepatic Alanine Aminotransferase Activity in *Clarias gariepinus* and *Oreochromis niloticus* Following Exposure to Oxybenzone.

Note: Values sharing identical superscript letters are considered statistically similar.

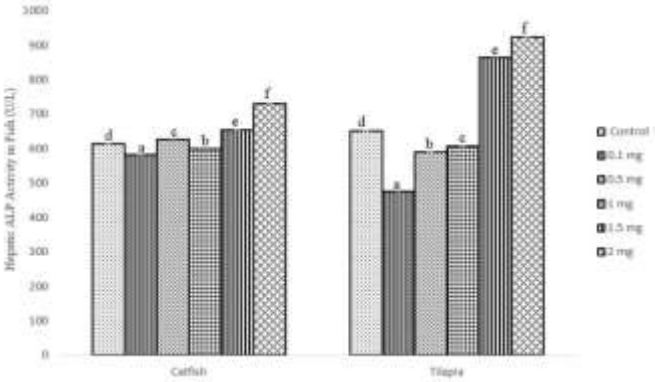

Figure 6: Hepatic Alkaline Phosphatase Activity in *Clarias gariepinus* and *Oreochromis niloticus* Following Exposure to Oxybenzone.

Values sharing identical superscript letters are considered statistically similar

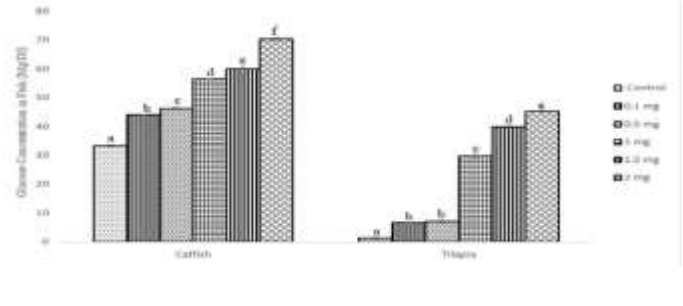

Figure 7: Glucose Concentration in *Clarias gariepinus* and *Oreochromis niloticus* in Response to Oxybenzone Exposure

Note: Values sharing identical superscript letters are considered statistically similar.

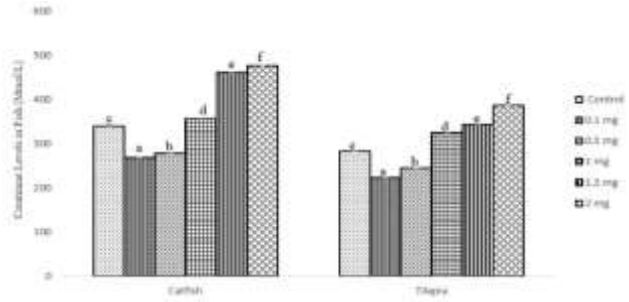

Figure 8: Creatinine Levels in *Clarias gariepinus* and *Oreochromis niloticus* After Exposure to Oxybenzone

Note: Values sharing identical superscript letters are considered statistically similar.

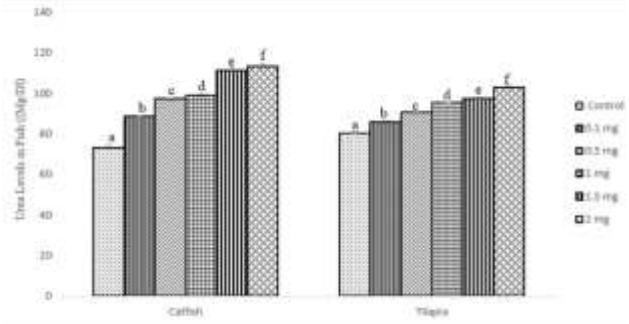

Figure 9: Urea Levels in *Clarias gariepinus* and *Oreochromis niloticus* Following Exposure to Oxybenzone Contamination

Note: Values sharing identical superscript letters are considered statistically similar.

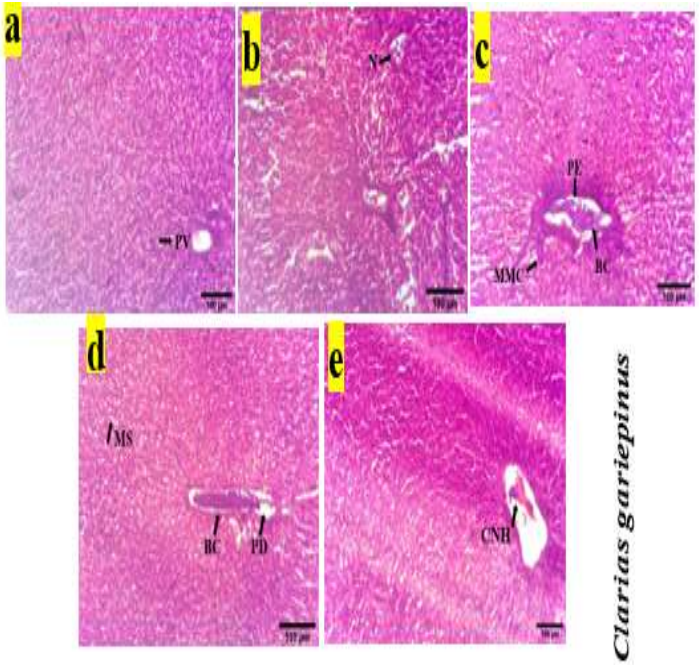

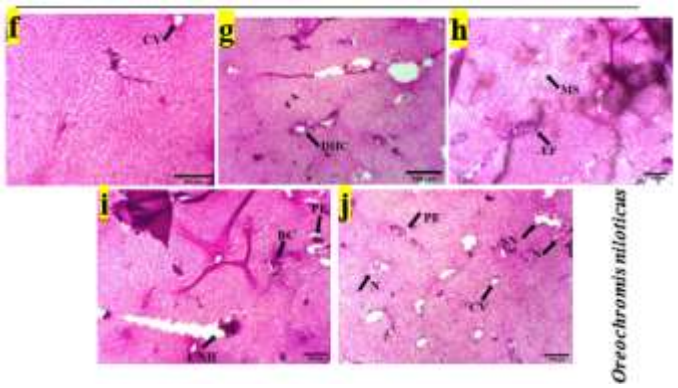

Plate 1. Histological analysis of fish liver sections showing (a) control liver of Clarias gariepinus with normal architecture and portal vein (PV), (b) necrosis (N) with disrupted tissue structure, (c) melano macrophage center (MMC), periportal edema (PE), and blood congestion (BC), (d) mild steatosis (MS) and patch degeneration (PD), (e) coagulative necrosis plus hemorrhage (CNH) with blood congestion (BC), (f) control liver of Oreochromis niloticus with central vein (CV), (g) diffuse hepatocyte congestion (DHC), (h) mild steatosis (MS) and extensive fibriosis (EF), (i) periportal edema (PE), blood congestion (BC), and coagulative necrosis plus hemorrhage (CNH), and (j) periportal edema (PE), necrosis (N), and central vein (CV). Scale bars = 100 µm.

Discussion

This study revealed that oxybenzone (OXB) induced significant oxidative stress in *C. gariepinus* and *O. niloticus*, evidenced by increases in hepatic superoxide dismutase (SOD) and glutathione peroxidase (GPx) activities. The observed increase in SOD activity maybe a compensatory response to neutralize the excessive generation of reactive oxygen species (ROS), since SOD catalyzes the dismutation of superoxide radicals (Zheng *et al*., 2023). *O. niloticus* exhibited higher baseline SOD activity and a more pronounced response at maximal OXB exposure (2 mg/L), which may suggest species specific capacity to process and manage antioxidant or metabolic stress from xenobiotics. In addition, it may also indicate a naturally robust antioxidant capacity in *O. niloticus*, potentially making it more resilient to oxidative stress. Similar induction in SOD activity as a result of exposure to UV filters was reported by Gayathri *et al.* (2023). They observed a significant elevation in SOD activity in embryonic zebrafish (*Danio rerio*) exposed to octocrylene (OC), at concentrations similar to what was deployed in this study (0.5 mg/L). Similarly, GPx activity, critical for detoxifying hydrogen peroxide and lipid hydroperoxides, and which are both byproducts of SOD activity and lipid peroxidation, respectively, was significantly induced in both species, further supporting the activation of antioxidant defenses (Temiz and Kargin, 2022). In similar fashion to the SOD activity, the stronger response of GPx activity in *O. niloticus* suggests it may have a more efficient glutathione-based antioxidant system, while *C. gariepinus* may rely more on other mechanisms to counteract oxidative stressors or have a threshold of which GPx induction cannot be breached.

Lipid peroxidation (LPO) serves as a key indicator of oxidative stress, reflecting the extent of ROS induced membrane damage in aquatic organisms. Variations in LPO levels among species highlight differences in metabolic rates, lipid composition, and susceptibility to oxidative damage. In this study, lipid peroxidation (LPO) levels in both species equally contrasted with oxidative damage, with *O. niloticus* exhibiting lesser baseline LPO levels, which can be likely due to inherent metabolic rates or lipid content. In contrast, *C. gariepinus* demonstrated steeper relative increases. The greater LPO in *C. gariepinus* suggests it is more susceptible to oxidative damage, possibly due to its lower baseline antioxidant capacity or less efficient repair mechanisms as observed with a threshold barred GPx induction, in comparison to *O. niloticus*. Another reason for this disparity in LPO induction could be attributed to the presence of scales on the skin of *O. niloticus*. Fish scales have the potential to counter lipid peroxidation due to their rich content of bioactive compounds, primarily collagen, peptides, and antioxidant minerals (Liu *et al*., 2024).

Aspartate aminotransferase (AST), alanine aminotransferase (ALT), and alkaline phosphatase (ALP) are core indicators of liver function widely used to detect and monitor hepatic injury. Elevated AST and ALT levels generally reflect hepatocellular membrane disruption, while increased ALP often points to cholestasis or biliary dysfunction (Lala et al., 2023). Together, these biomarkers provide critical insights into the nature and extent of liver damage, guiding both diagnostic assessments and therapeutic interventions. The inhibition of the ALT and ALP enzymes at lower concentrations may indicate early stage metabolic changes or protective mechanisms. However, the increase in both ALT and ALP at higher concentrations of OXB suggests that the liver is undergoing critical impairment (Lala et al., 2023). AST and ALT, released during hepatocyte membrane disruption, were significantly higher in *O. niloticus* at equivalent concentrations, which can be adduced to greater metabolic sensitivity or higher hepatic enzyme activity. Findings from this study align with a previous study which reported that zinc oxide nanoparticles increased AST and ALT activities of the liver in serum of crucian carp (*Carassius carassius*) (Hong *et al*., 2022). ALP increases linked to cholestasis were most pronounced in *O. niloticus* at 2 mg/L, highlighting species dependent biliary dysfunction. Furthermore, ALP enzyme's activity is often a sign of cellular or tissue injury and is linked to protein metabolism changes in aquatic species subjected to ecological stress (Kerdgari *et al*., 2022).

Glucose levels serve as a key indicator of metabolic and stress responses; disruptions in glucose homeostasis may be an indication of impaired energy balance and increased gluconeogenesis linked to stress, most probably via peripheral proteolysis (Han et al., 2016). The induced hyperglycemia observed in both *C. gariepinus* and *O. niloticus*, may likely reflects stress-induced gluconeogenesis due to catecholamines acting on liver and tissue glycogen centers (Renitasari *et al*., 2021). This high synthesis of glucose in fish was corroborated by a previous study by Goda *et al*. (2023). They reported high glucose levels in tilapia fish exposed to the UV filter zinc oxide nanoparticles (ZnO-NPs). Renal dysfunction was evident through hightened levels of urea and creatinine, both biomarkers of impaired glomerular filtration. Notably, *C. gariepinus* exhibited higher creatinine and urea levels than *O. niloticus* at comparable concentrations, which implies greater nephrotoxic susceptibility or intrinsic physiological differences. These findings also align with Shahzadi *et al*. (2024), who observed significantly elevated creatinine and urea levels in carbofuran-exposed fish (*Labeo rohita*).

Histopathological analysis serves as a important diagnostic tool in aquatic toxicology, providing direct visualization of cellular damage that reveals both the mechanisms and progression of tissue toxicity. In *C. gariepinus*, hepatocellular damage manifested through coagulative necrosis with hemorrhage (CNH) and melano-macrophage center (MMC) formation. The CNH pattern may be an indication of severe ischemic or cytotoxic injury (Wolf et al., 2014). Concurrent MMCs, consisting of pigment-laden macrophages, signify chronic inflammatory processes resulting from either persistent toxin exposure or impaired debris clearance (Agius & Roberts, 2003). This combination may imply a biphasic injury pattern where necrotic events trigger sustained immune activation. *O. niloticus* presented a contrasting response dominated by diffuse hepatocyte congestion (DHC) and extensive fibriosis (EF). The generalized sinusoidal erythrocyte pooling (DHC) implies a circulatory compromise, while EF represents an attempted healing response through extracellular matrix deposition. Importantly, fibrogenesis initially functions as a transient repair mechanism, facilitating tissue scaffolding for regeneration before matrix resorption during resolution (Hanquier et al., 2023). However, persistent toxic insults can disrupt this balance, leading to pathological fibrosis as observed in our specimens. Common vascular disturbances in both species, particularly periportal edema (PE) and blood congestion (BC), likely stem from a toxicant induced endothelial damage and hypoxia (Wolf & Wheeler, 2018). These changes may precede and exacerbate parenchymal injury by compromising the hepatic microcirculation. The presence of mild steatosis (MS) across both species further indicates metabolic disruption, potentially through toxin interference with β-oxidation or lipoprotein export (Jia et al., 2020). The divergent histopathological trajectories of both species may reflect differences in antioxidant defenses, detoxification efficiency, and immune modulation.

Conclusions

This study shows that oxybenzone (OXB) triggers significant oxidative stress and systemic toxicity in *C. gariepinus* and *O. niloticus*, with clear differential in the response of the test organisms. The significant elevation in hepatic SOD and GPx activities reveal activated antioxidant defenses against ROS synthesis. *O. niloticus* mounted a stronger antioxidant response, likely due to its higher baseline SOD and efficient glutathione system. In contrast, *C. gariepinus* showed limited GPx induction, hinting at weaker or alternative defense mechanisms. Lipid peroxidation levels pointed to greater oxidative damage in *C. gariepinus*, possibly linked to its lower antioxidant reserves and lack of protective scales, unlike *O. niloticus*, whose scales may help shield against lipid damage. The concurrent alterations in SOD, GPx, and LPO levels establish a clear correlation between antioxidant enzyme responses and oxidative stress biomarkers, suggesting that these biochemical parameters can serve as reliable indicators of OXB-induced oxidative stress in fish species. Hepatic injury indicators (AST, ALT, ALP) showed higher metabolic sensitivity in *O. niloticus*, while renal dysfunction (elevated urea and creatinine) was more severe in *C. gariepinus*. Stress induced hyperglycemia and energy metabolism disruptions were noted in both species. Histopathology results confirmed vascular and metabolic damage with *C. gariepinus* displaying blood congestion, while *O. niloticus* developed progressive fibrosis. The result from this study underlines the need to account for species specific physiology when evaluating ecological risks of chemical pollutants like UV filters. Future research should dive deeper into the molecular mechanisms behind these divergent responses.

Declarations

Acknowledgements
The authors wish to express their sincere gratitude to Mr. Festus O. Igbe and Mr. Umar H. I for their assistance with the biochemical assays and to Mrs. Elizabeth T. Ojo for her support in providing essential laboratory equipment and guidance throughout the laboratory sessions.

References

Adeyemi, J. A., Ogunwole, G. A., Bamidele, O. S., & Adedire, C. O. (2022). Effects of pre-treatment with waterborne selenium on redox homeostasis and humoral innate immune parameters in African catfish (Clarias gariepinus) experimentally challenged with Serratia marcescens. Fish Physiology and Biochemistry, 48(2), 409–418.

Agius, C., & Roberts, R. J. (2003). Melano-macrophage centres and their role in fish pathology. Journal of Fish Diseases, 26(9), 499–509. https://doi.org/10.1046/j.1365-2761.2003.00485.x

Ajeniyi, S. A., & Solomon, R. J. (2014). Urea and creatinine of Clarias gariepinus in three different commercial ponds. Nature and Science, 12(10), 124–138. http://www.sciencepub.net/nature

Bai, C., Dong, H., Tao, J., Chen, Y., Xu, H., Lin, J., Huang, C., & Dong, Q. (2023). Lifetime exposure to benzophenone-3 at an environmentally relevant concentration leads to female-biased social behavior and cognition deficits in zebrafish. Science of the Total Environment, 857, 159733. https://doi.org/10.1016/j.scitotenv.2022.159733

Balmer, M. E., Buser, H. R., Müller, M. D., & Poiger, T. (2005). Occurrence of some organic UV filters in wastewater, in surface waters, and in fish from Swiss lakes. Environmental Science & Technology, 39, 953–962.

Bratkovics, S., Wirth, E., Sapozhnikova, Y., Pennington, P., & Sanger, D. (2015). Baseline monitoring of organic sunscreen compounds along South Carolina's coastal marine environment. Marine Pollution Bulletin, 101, 370–377. https://doi.org/10.1016/j.marpolbul.2015.10.015

Chatzigianni, M., Pavlou, P., Siamidi, A., Vlachou, M., Varvaresou, A., & Papageorgiou, S. (2022). Environmental impacts due to the use of sunscreen products: A mini-review. Ecotoxicology, 31(9), 1331–1345. https://doi.org/10.1007/s10646-022-02592-w

Clara-Bindu, F., Anila, P. A., Sutha, J., & Ramesh, M. (2021). Sub-lethal toxicity of alphamethrin on biochemical indices in a freshwater fish, Cyprinus carpio. International Journal of Fisheries and Aquatic Studies, 9(1), 414–419. https://doi.org/10.22271/fish.2021.v9.i1e.2428

Dinardo, J., & Downs, C. (2021). Failure to protect: Do sunscreens prevent skin cancer in humans? ResearchGate.

Dorcas, I. K., & Solomon, R. J. (2014). Calculation of liver function test in Clarias gariepinus collected from three commercial fish ponds. Nature and Science, 12(10), 107–123. http://www.sciencepub.net/nature

Downs, C. A., Kramarsky-Winter, E., Segal, R., Fauth, J., Knutson, S., Bronstein, O., … Loya, Y. (2016). Toxicopathological effects of the sunscreen UV filter oxybenzone (benzophenone-3) on coral planulae and cultured primary cells and its environmental contamination in Hawaii and the U.S. Virgin Islands. Archives of Environmental Contamination and Toxicology. https://doi.org/10.1007/s00244-015-0227-7

Esenowo, L. K., Nelson, A. U., Ekpo, N. D., Chukwu, M. N., Akpan, A. U., Ugwumba, A. A. A., … Oboho, D. E. (2022). Effects of acute exposure to chlorfenapyr on hepatic enzyme activities and serum lipid profile of African catfish (Clarias gariepinus). World Journal of Applied Science and Technology, 14(1b), 86–93. https://doi.org/10.4314/wojast.v14i1b.86

García-Márquez, M. G., Rodríguez-Castañeda, J. C., & Agawin, N. S. R. (2024). Effects of the sunscreen ultraviolet filter oxybenzone (benzophenone-3) on the seagrass Posidonia oceanica and its associated N_2 fixers. Science of the Total Environment, 918, 170751. https://doi.org/10.1016/j.scitotenv.2024.170751

Gayathri, M., Sutha, J., Mohanthi, S., Ramesh, M., & Poopal, R. K. (2023). Ecotoxicological evaluation of the UV-filter octocrylene in embryonic zebrafish (Danio rerio). Comparative Biochemistry and Physiology Part C: Toxicology & Pharmacology, 271, 109688. https://doi.org/10.1016/j.cbpc.2023.109688

Goda, M. N., Shaheen, A. A. M., & Hamed, H. S. (2023). Potential role of dietary parsley and/or parsley nanoparticles against zinc oxide nanoparticles toxicity-induced physiological and histological alterations in Nile tilapia. Aquaculture Reports, 28, 101425. https://doi.org/10.1016/j.aqrep.2022.101425

Han, H. S., Kang, G., Kim, J., et al. (2016). Regulation of glucose metabolism from a liver-centric perspective. Experimental & Molecular Medicine, 48, e218. https://doi.org/10.1038/emm.2015.122

Hanquier, Z., Misra, J., Baxter, R., & Maiers, J. L. (2023). Stress and liver fibrogenesis. American Journal of Pathology, 193(10), 1363–1376. https://doi.org/10.1016/j.ajpath.2023.06.006

Hong, H., Liu, Z., Li, S., Wu, D., Jiang, L., Li, P., Wu, Z., Xu, J., Jiang, A., Wei, Z., & Yang, Z. (2022). Zinc oxide nanoparticles (ZnO-NPs) exhibit immune toxicity to crucian carp (Carassius carassius) by neutrophil extracellular traps (NETs) release and oxidative stress. Fish & Shellfish Immunology, 129, 22–29. https://doi.org/10.1016/j.fsi.2022.07.025

Ikumawoyi, V., Awodele, O., Rotimi, K., & Fashina, Y. (2016). Evaluation of the effects of the hydro-ethanolic root extract of Zanthoxylum zanthoxyloides on hematological parameters and oxidative stress in cyclophosphamide-treated rats. African Journal of Traditional, Complementary and Alternative Medicines, 13(5), 153–159.

Jia, R., Cao, L. P., Du, J. L., He, Q., Gu, Z. Y., Jeney, G., Xu, P., & Yin, G. J. (2020). Effects of high-fat diet on steatosis, endoplasmic reticulum stress, and autophagy in the liver of tilapia (Oreochromis niloticus). Frontiers in Marine Science, 7, 363. https://doi.org/10.3389/fmars.2020.00363

Kerdgari, M., Afkhami, M., Ehsanpour, M., & Ghanbarzadeh, M. (2022). Monitoring anthropogenic pollutants in northern coasts of Hormuz Strait using blood indices and thyroid hormone levels in Periophthalmus argentilineatus (Pisces: Gobiidae). Iranian Journal of Fisheries Sciences, 21, 431–444.

Labille, J., Slomberg, D., Catalano, R., Robert, S., Apres-Termelo, M. L., Boudenne, J. L., Manasfi, T., & Radakovitch, O. (2020). Assessing UV filter inputs into beach waters during recreational activity: A field study of three French Mediterranean beaches

from consumer survey to water analysis. Science of the Total Environment, 706, 136010. https://doi.org/10.1016/j.scitotenv.2019.136010

Lala, V., Zubair, M., & Minter, D. A. (2025). Liver function tests. In StatPearls [Internet]. StatPearls Publishing. https://www.ncbi.nlm.nih.gov/books/NBK482489/

Liu, X., Hu, Q., Shen, Y., Wu, Y., Gao, L., Xu, X., & Hao, G. (2024). Research progress on antioxidant peptides from fish by-products: Purification, identification, and structure–activity relationship. Metabolites, 14(10), 561. https://doi.org/10.3390/metabo14100561

Mao, F., He, Y., & Gin, K. (2018). Occurrence and fate of benzophenone-type UV filters in aquatic environments: A review. Environmental Science: Water Research & Technology, 5, 209–222. https://doi.org/10.1039/C8EW00539G

Marcin, S., & Aleksander, A. (2023). Acute toxicity assessment of nine organic UV filters using a set of biotests. Toxicological Research, 39(4), 649–667. https://doi.org/10.1007/s43188-023-00192-2

Mustieles, V., Balogh, R. K., Axelstad, M., Montazeri, P., Márquez, S., Vrijheid, M., Draskau, M. K., Taxvig, C., Peinado, F. M., Berman, T., Frederiksen, H., Fernández, M. F., Vinggaard, A. M., & Andersson, A. M. (2023). Benzophenone-3: Comprehensive review of the toxicological and human evidence with meta-analysis of human biomonitoring studies. Environment International, 173, 107739. https://doi.org/10.1016/j.envint.2023.107739

Nwabueze, J. C., Sogbanmu, T. O., & Ugwumba, A. A. (2020). Physicochemical characteristics, animal species diversity, and oxidative stress responses in dominant fish from an impacted site on the Lagos Lagoon, Nigeria. Ife Journal of Science, 22(2), 81–93.

Ogunwole, G. A., Adeyemi, J. A., Saliu, J. K., & Olorundare, K. E. (2024). A computational analysis of the molecular mechanisms underlying the effects of ibuprofen and dibutyl phthalate on gene expression in fish. Heliyon, 10(11), e31880. https://doi.org/10.1016/j.heliyon.2024.e31880

Ortiz-Román, M. I., Casiano-Muñiz, I. M., & Román-Velázquez, F. R. (2024). Toxicity of UV filter benzophenone-3 in brine shrimp nauplii (Artemia salina) and zebrafish (Danio rerio) embryos. Journal of Xenobiotics, 14, 537–553. https://doi.org/10.3390/jox14020032

Pham, D. N., Sokolov, E. P., Falfushynska, H., & Sokolova, I. M. (2022). Gone with sunscreens: Responses of blue mussels (Mytilus edulis) to a wide concentration range of a UV filter ensulizole. Chemosphere, 309, 136736. https://doi.org/10.1016/j.chemosphere.2022.136736

Renitasari, D. P., Kurniawan, A., & Kurniaji, A. (2021). Blood glucose of tilapia fish (Oreochromis mossambica) as a water bioindicator in the downstream of Brantas Waters, East Java. Aquaculture, Aquarium, Conservation & Legislation – Bioflux, 14(4).

Santonocito, M., Salerno, B., Trombini, C., Tonini, F., Pintado-Herrera, M. G., Martínez-Rodríguez, G., & Hampel, M. (2020). Stress under the sun: Effects of exposure to low concentrations of UV-filter 4-methylbenzylidene camphor (4-MBC) in a marine bivalve filter feeder, the Manila clam (Ruditapes philippinarum). Aquatic Toxicology, 221, 105418. https://doi.org/10.1016/j.aquatox.2020.105418

Shahzadi, M., Ahmad, M., Rafique, H., Akmal, H., Ditta, A., Ali, S., Akram, I., & Shahzad, K. (2024). Protective effects of Moringa oleifera against carbofuran-induced toxicity in fish (Labeo rohita): Insight into hematobiochemical, histology, oxidative, and antioxidant biomarkers. Kuwait Journal of Science, 51(3), 100249. https://doi.org/10.1016/j.kjs.2024.100249

Statista Search Department. (2022). Market revenue of the sun protection market worldwide from 2013 to 2026 [Infographic]. Statista. https://www.statista.com/forecasts/812522/sun-care-market-value-global

Suh, S., Pham, C., Smith, J., & Mesinkovska, N. A. (2020). The banned sunscreen ingredients and their impact on human health: A systematic review. International Journal of Dermatology, 59(9), 1033–1042. https://doi.org/10.1111/ijd.14824

Tao, J., Yang, Q., Jing, M., Sun, X., Tian, L., Huang, X., Huang, X., Wan, W., Ye, H., Zhang, T., & Hong, F. (2023). Embryonic benzophenone-3 exposure inhibited fertility in later-life female zebrafish and altered developmental morphology in offspring embryos. Environmental Science and Pollution Research International. https://doi.org/10.1007/s11356-023-25843-7

Temiz, O., & Kargin, F. (2022). Toxicological impacts on antioxidant responses, stress protein, and genotoxicity parameters of aluminum oxide nanoparticles in the liver of Oreochromis niloticus. Biological Trace Element Research, 200, 1339–1346. https://doi.org/10.1007/s12011-021-02723-0

Thomas, T., Fat, M., & Kearns, G. (2024). Sunscreens: Potential hazards to environmental and human health. Frontiers in Marine Science, 11, 1471574. https://doi.org/10.3389/fmars.2024.1471574

Wang, Y., Jiang, S., Chan, X., Liu, X., Li, N., Nie, Y., & Lu, G. (2023). Comparison of developmental toxicity of benzophenone-3 and its metabolite benzophenone-8 in zebrafish. Aquatic Toxicology, 258, 106515. https://doi.org/10.1016/j.aquatox.2023.106515

Wolf, J. C., Baumgartner, W. A., Blazer, V. S., Camus, A. C., Engelhardt, J. A., Fournie, J. W., Frasca, S., Jr., Groman, D. B., Kent, M. L., Khoo, L. H., Law, J. M., Lombardini, E. D., Ruehl-Fehlert, C., Segner, H. E., Smith, S. A., Spitsbergen, J. M., Weber, K., & Wolfe, M. J. (2014). Toxicologic Pathology. Toxicologic Pathology. Advance online publication. https://doi.org/10.1177/0192623314540229

Wolf, J. C., & Wheeler, J. R. (2018). A critical review of histopathological findings associated with endocrine and non-endocrine hepatic toxicity in fish models. Aquatic Toxicology, 197, 60–78. https://doi.org/10.1016/j.aquatox.2018.01.013

Zhao, G., Gao, M., Guo, S., Zeng, S., Ye, C., Wang, M., & Hong, Y. (2023). UV filter ethylhexyl salicylate affects cardiovascular development by disrupting lipid metabolism in zebrafish embryos. Science of the Total Environment, 164073. https://doi.org/10.1016/j.scitotenv.2023.164073

Zheng, M., Liu, Y., Zhang, G., Yang, Z., Xu, W., & Chen, Q. (2023). The applications and mechanisms of superoxide dismutase in medicine, food, and cosmetics. Antioxidants, 12(9), 1675. https://doi.org/10.3390/antiox12091675

Zhou, R., Lu, G., Yan, Z., Jiang, R., Sun, Y., & Zhang, P. (2022). Epigenetic mechanisms of DNA methylation in the transgenerational effect of ethylhexyl salicylate on zebrafish. Chemosphere, 295, 133926. https://doi.org/10.1016/j.chemosphere.2022.133926

Ziaei-Nejad, S., Hosseini, S. M., & Seyed Mortezaei, S. R. (2021). Effects of selenium nanoparticles supplemented feed on biochemical indices, growth and survival of yellow-tail seabream (Acanthopagrus latus). Journal of Agricultural Science and Technology, 23(5), 1001–1011.